It is obvious that formula I, which assumes that the stoichiometric number of hydroxides is necessary for lattice stability, is in error. Also in apparent error is formula II that assumes only X-type vacancies over the entire range $0 \leq X \leq 2$. A similar conclusion can be made about the compositional formulas that are restricted to Ca/P molar ratios either greater than 1.50 (formula V) or less than 1.50 (formula VI). Formula VI makes the further assumption that at least one hydroxide ion must be present for lattice stability, yet it is apparent that many DHAs were prepared with less than one hydroxide per unit cell.

It is interesting that the number of X-type vacancies tended to decrease as the Ca/P ratio increased whereas the number of Y-type vacancies remained relatively constant at a value of approximately 0.5 per unit cell. This may explain why the DHAs prepared under mild aqueous conditions appeared able to only incorporate about half the maximum amount of hydroxide ion in the crystal lattice. It is impossible to determine, however, whether structural constraints initially excluded the calcium or the hydroxide ions from their positions in the lattice, resulting in the loss of an electrically equivalent amount of the counterion. X-Type vacancies were most prevalent in precipitates formed at lower pH. This was probably reflective of the chemical environment in which the crystalline phases were formed, which was relatively higher in acid phosphate and lower in hydroxide ion and consequently may not be related to the structural requirements of the DHAs.

Another interesting feature of the data in Table IV, often ignored in the consideration of the structure of DHAs, is the presence of a considerable amount of water in the lyophilized samples. On a molecular basis, the number of water molecules is comparable to that of the phosphate ions, which are generally thought to be primarily responsible for maintaining structural integrity of the apatite lattice.[41] The high surface areas of these DHAs ($\sim$130–170 m^2/g) could easily accommodate a considerable portion of the water; nevertheless, even small amounts of the water in the lattice could interfere with filling of the hydroxide and/or calcium vacancies and result in the observed vacancy in at least half the hydroxide positions. Contractions in the *a*-axis dimensions of the DHAs heated in the 200–400 °C range have been correlated with dehydration and loss of structural water.[42]

The complete chemical compositions of the DHAs reported here were compared to various defect apatite formulas, and possible structural defects in their apatite lattices were inferred on the basis of a lattice model composed of stoichiometric HA with a negligible surface contribution. The large surface contributions of about 130–170 m^2/g for these small-size DHAs and the unknown extent of compositional and structural coherence at their surfaces cause uncertainty in the degree of structural imperfection and defects inferred. With neglect of surface contributions, the implicated degree of defects in the DHAs studied here with Ca/P ratios greater than 1.5 is conceptually more realistic than that with ratios considerably less than 1.5. It may be difficult for a HA lattice to maintain its structural integrity with the degree of inferred structural defects for the DHAs with Ca/P ratios much less than 1.5. A less defect and more structurally integral model in this low Ca/P ratio region is a partially hydrolyzed OCP lattice or interlayered OCP–HA lattice.[43]

Acknowledgment. The authors wish to thank A. W. Hailer for his valuable technical assistance.

Registry No. Hydroxylapatite, 1306-06-5.

(41) Elliott, J. C. *Clin. Orthop. Relat. Res.* **1973**, *93*, 313.
(42) LeGeros, R. Z.; Bonel, G.; Legros, R. *Calcif. Tissue Res.* **1978**, *26*, 111.
(43) Brown, W. E.; Smith, J. P.; Lehr, J. R.; Frazier, A. W. *Nature (London)* **1962**, *196*, 1050.

Contribution from the Department of Chemistry, Florida Atlantic University, Boca Raton, Florida 33431

Eight-Coordinate Complexes of Molybdenum with 1,1-Dithio Ligands. Correlation of Redox Potentials with Ligand Substituent Parameters and Spectroscopic Properties

DORIS A. SMITH and FRANKLIN A. SCHULTZ*

Received November 17, 1981

Electrochemical half-wave potentials and charge-transfer absorption, EPR, and X-ray photoelectron spectral properties are reported for a series of eight-coordinate molybdenum complexes with dithiocarbamate, thioxanthate, and 1,1-disubstituted ethylenedithiolate ligands. The complexes undergo reversible Mo(VI)/Mo(V) and Mo(V)/Mo(IV) electron transfers with $E_{1/2}$ for a given charge-transfer step spanning a range of 2 V for the ligands studied. Shifts in $E_{1/2}$ are correlated successfully with parameters expressing the electron-donating or -withdrawing capabilities of ligand substituent groups. Charge-transfer absorption energies and Mo(V) EPR spectral properties experience relatively little change with ligand structure. However, Mo 3d and S 2p XPE binding energies exhibit significant changes with ligand structure and correlate well with electrochemical half-wave potentials. Results are interpreted in terms of a qualitative molecular orbital model for eight-coordinate Mo(VI), -(V), and -(IV) complexes in which reversible electron transfers occur within a d_{xy} orbital of nearly pure metal character. The energy of this orbital increases or decreases in response to the amount of negative charge inductively donated from the ligands to the metal through orbitals not involved in the electrochemical charge-transfer process. However, the character of the Mo d_{xy} orbital and its position relative to other orbitals in the molecular manifold appear to change very little as ligand structure is varied.

Introduction

Interest in the chemistry of molybdenum complexes with sulfur-containing ligands arises from the knowledge that extensive Mo–S bonding occurs in molybdenum-containing enzymes.[1] Dithio acid and 1,1-dithiolate ligands[2-4] provide transition metals with a sulfur-rich coordination environment. Mononegative dithiocarbamate,[4-8] dithiobenzoate,[9,10] and

(1) For a recent review, see: Stiefel, E. I. In "Molybdenum and Molybdenum-Containing Enzymes", Coughlan, M. P., Ed.; Pergamon Press: Oxford, 1980; Chapter 2.
(2) Coucouvanis, D. *Prog. Inorg. Chem.* **1970**, *11*, 233.
(3) Coucouvanis, D. *Prog. Inorg. Chem.* **1979**, *26*, 301.
(4) Willemse, J.; Cras, J. A.; Steggerda, J. J.; Keijzers, C. P. *Struct. Bonding (Berlin)* **1976**, *28*, 83.
(5) Nieuwpoort, A. Ph.D. Thesis, University of Nijmegen, The Netherlands, 1975.
(6) Nieuwpoort, A.; Steggerda, J. J. *Recl. Trav. Chim. Pays-Bas* **1976**, *95*, 250.

0020-1669/82/1321-3035$01.25/0 © 1982 American Chemical Society

thioxanthate[11] ligands form tetrakis complexes with molybdenum, thereby generating an MoS_8 coordination shell.

In a forthcoming paper[12] we report the preparation and characterization of a new series of eight-coordinate molybdenum complexes containing the dinegative ethylenedithiolate (ed) ligands 1,1-dicyano-2,2-ethylenedithiolate (*i*-mnt), 1-cyano-1-carbethoxy-2,2-ethylenedithiolate (ced), and 1,1-dicarbethoxy-2,2-ethylenedithiolate (ded). These complexes together with previously reported species containing *N,N*-diethyldithiocarbamate (Et_2dtc)[5,6] and *tert*-butyl thioxanthate (*t*-Butxn)[11] ligands comprise a family of structurally similar compounds that displays an interestingly large range of redox potentials and distinctive spectroscopic properties. In the present paper we report on the electrochemical and visible absorption, EPR, and X-ray photoelectron (XPE) spectroscopic properties of these compounds and examine correlations of their half-wave potentials with spectroscopic and ligand substituent parameters. These correlations illustrate important relationships among redox potentials, spectroscopic properties, and ligand structure in transition metal complexes which are brought clearly into focus by unique electronic and structural features of the MoS_8 complexes.

Experimental Section

Materials. Synthetic procedures and characterization of the Mo(V) complexes $(n\text{-}Bu_4N)_3Mo(i\text{-}mnt)_4$, $(n\text{-}Bu_4N)_3Mo(ced)_4$, $(n\text{-}Pr_4N)_3Mo(ded)_4$, and $Mo(Et_2dtc)_4PF_6$ are described in ref 12. Solutions of $Mo(t\text{-}Butxn)_4^+$ were prepared by chemical or electrochemical oxidation of $Mo(t\text{-}Butxn)_4$.[11] We were unable to isolate a pure solid sample of a $Mo(t\text{-}Butxn)_4^+$ salt as had been reported for $Mo(i\text{-}Prtxn)_4PF_6$.[11]

Solvents for electrochemical and spectroscopic studies were Aldrich spectrophotometric grade acetonitrile and dichloromethane; these were stored over activated molecular sieves. The supporting electrolytes in electrochemical experiments were tetraethylammonium tetrafluoroborate. ($(TEA)BF_4$) and tetra-*n*-butylammonium hexafluorophosphate ($(TBA)PF_6$) from Southwestern Analytical Chemicals.

Equipment and Procedures. Equipment and procedures for cyclic voltammetric and thin-layer spectroelectrochemical experiments are described in ref 12. Electronic spectral data from 350 to 700 nm were obtained in a thin-layer spectroelectrochemical cell under potentiostatic control using a Harrick RSS-C rapid-scan spectrophotometer. Electronic spectral data from 570 to 900 nm were obtained with Cary 14 and Perkin-Elmer 575 spectrophotometers. For generation of molybdenum(VI) ethylenedithiolate complexes for these latter measurements, dichloromethane solutions of $Mo(i\text{-}mnt)_4^{3-}$, $Mo(ced)_4^{3-}$, and $Mo(ded)_4^{3-}$ were oxidized with Br_2, Br_2, and I_2, respectively.

Room-temperature EPR spectra of dichloromethane solutions of the isolated Mo(V) complexes were recorded at 9.52 GHz with a Varian Model 4502 spectrometer.[13] The EPR spectrum of $Mo(t\text{-}Butxn)_4^+$ was acquired after oxidizing a solution of $Mo(t\text{-}Butxn)_4$ in CH_2Cl_2 with Br_2.

XPE spectra were recorded on a Physical Electronics Industries Model 548 AR spectrometer at The University of North Carolina, Chapel Hill, NC.[14] Samples were run as powders pressed into indium foil. Measurements were made at low X-ray flux and maximum instrument resolution. There was no evidence for decomposition of any of the samples during the measurements.

Results

Electrochemistry. Interest in the electrochemical behavior of the MoS_8 complexes arises from the considerable influence of ligand structure on redox potentials as evident from earlier studies of the dithiocarbamate[5,6] and thioxanthate[11] complexes. Figure 1 shows cyclic voltammetric traces recorded in CH_3CN for all five of the eight-coordinate complexes starting in the Mo(V) oxidation state.

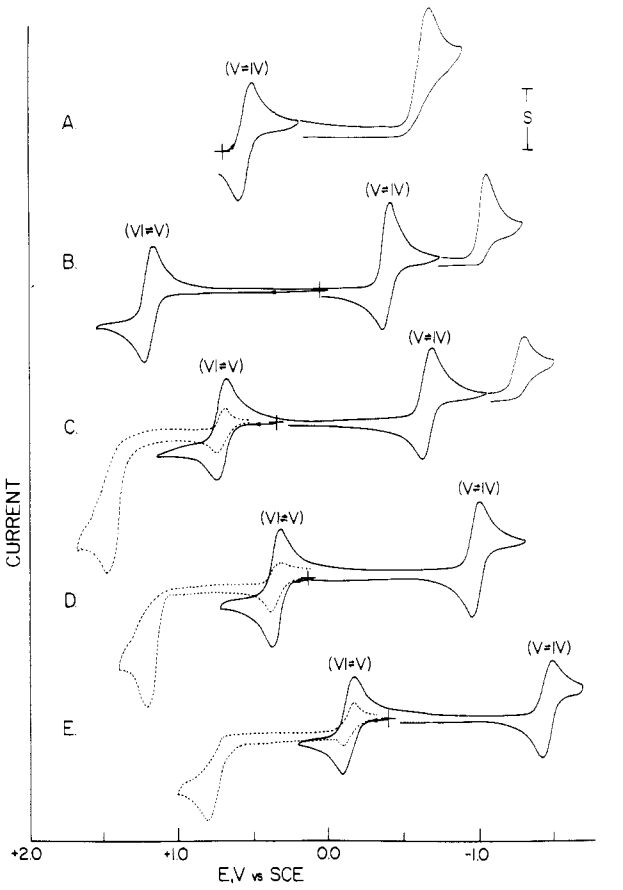

Figure 1. Cyclic voltammetric traces for MoS_8 complexes in 0.1 M $(TEA)BF_4/CH_3CN$: A, $Mo(t\text{-}Butxn)_4^+$, unknown concentration, v = 50 mV s^{-1}; B, 1.07 mM $Mo(Et_2dtc)_4^+$, v = 50 mV s^{-1}, S = 10 μA; C, 1.07 mM $Mo(i\text{-}mnt)_4^{3-}$, v = 50 mV s^{-1}, S = 10 μA; D, 0.23 mM $Mo(ced)_4^{3-}$, v = 100 mV s^{-1}, S = 2.5 μA; E, 0.22 mM $Mo(ded)_4^{3-}$, v = 100 mV s^{-1}, S = 5 μA. Broken lines were recorded at half the indicated current sensitivity.

Four of the five Mo(V) complexes ($Mo(t\text{-}Butxn)_4^+$ excepted) exhibit a reversible oxidation, which is designated wave 1. All five Mo(V) complexes exhibit a reversible reduction, which is designated wave 2. On the basis of cyclic voltammetric peak current parameters, peak current ratios, and peak potential separations and results from controlled-potential coulometric (CPC) and thin-layer spectroelectrochemical experiments,[12] waves 1 and 2 are judged to be reversible one-electron transfers. The one-electron nature of waves 1 and 2 is confirmed by the CPC oxidations of $Mo(ded)_4^{3-}$, $Mo(ced)_4^{3-}$, $Mo(i\text{-}mnt)_4^{3-}$, and $Mo(Et_2dtc)_4^+$ (corresponding to wave 1) and of $Mo(t\text{-}Butxn)_4$ (corresponding to wave 2), which yield values of n = 1.02, 1.00, 1.02, 0.95, and 0.99, respectively. The oxidation products are stable and can be reduced quantitatively to the original complex with the exception of $Mo(Et_2dtc)_4^{2+}$, which undergoes partial (~15%) decomposition in CH_3CN. At more extreme potentials the Mo(VI) forms of the *i*-mnt, ced, and ded complexes undergo an irreversible oxidation, designated wave A, and the Mo(IV) forms of the *t*-Butxn, Et_2dtc, and *i*-mnt complexes undergo an irreversible reduction, designated wave C. Voltammetric redox potentials for waves 1, 2, A, and C in CH_3CN and CH_2Cl_2 are collected in Table I. Detailed electrochemical characterization of these processes is presented in ref 12.

(7) Nieuwpoort, A.; Steggerda, J. J. *Recl. Trav. Chim. Pays-Bas* **1976**, *95*, 289.
(8) Nieuwpoort, A.; Steggerda, J. J. *Recl. Trav. Chim. Pays-Bas* **1976**, *95*, 294.
(9) Piovesana, O.; Sestili, L. *Inorg. Chem.* **1974**, *13*, 2745.
(10) Roberie, T.; Hoberman, A. E.; Selbin, J. *J. Coord. Chem.* **1979**, *9*, 79.
(11) Hyde, J.; Zubieta, J. *J. Inorg. Nucl. Chem.* **1977**, *39*, 289.
(12) Smith, D. A.; McDonald, J. W.; Ott, V. R.; Finklea, H. O.; Schultz, F. A. *Inorg. Chem.*, in press.
(13) We thank Dr. J. W. McDonald of the Charles F. Kettering Research Laboratory, Yellow Springs, Ohio, for making these measurements.
(14) We thank Dr. M. Umaña and Mr. D. Griffis for their assistance in obtaining and interpreting these spectra.

Table I. Voltammetric Redox Potentials (V vs. SCE)

complex	$(E_p)_A$[b]	$(E_{1/2})_1$[a]	$(E_{1/2})_2$[a]	$(E_p)_C$[b]
		Acetonitrile (0.2 M (TEA)BF_4)		
Mo(*t*-Butxn)$_4^+$			+0.494	−0.730
Mo(Et_2dtc)$_4^+$		+1.152	−0.444	−1.141
Mo(*i*-mnt)$_4^{3-}$	+1.433	+0.654	−0.715	−1.295
Mo(ced)$_4^{3-}$	+1.208	+0.304	−1.024	
Mo(ded)$_4^{3-}$	+0.800	−0.132	−1.472	
		Dichloromethane (0.1 M (TBA)PF_6)		
Mo(*t*-Butxn)$_4^+$			+0.369	−0.953
Mo(Et_2dtc)$_4^+$		+1.129	−0.550	−1.283
Mo(*i*-mnt)$_4^{3-}$	+1.510	+0.519	−0.843	−1.723
Mo(ced)$_4^{3-}$	+1.060	+0.175	−1.178	
Mo(ded)$_4^{3-}$	+0.830	−0.302	−1.672	

[a] Reversible half-wave potential; determined from $E_{1/2} = (E_{pc} + E_{pa})/2$ at sweep rates of 0.02–0.2 V s^{-1}. [b] Irreversible peak potential measured at 0.1 V s^{-1}.

Table II. EPR Spectral Data[a]

complex	g	A, $cm^{-1} \times 10^4$	complex	g	A, $cm^{-1} \times 10^4$
Mo(*t*-Butxn)$_4^+$[b]	1.981	30.4	Mo(ced)$_4^{3-}$	1.982	32.0
Mo(Et_2dtc)$_4^+$	1.980	34.1	Mo(ded)$_4^{3-}$	1.983	32.2
Mo(*i*-mnt)$_4^{3-}$	1.979	32.7			

[a] In CH_2Cl_2 at room temperature. [b] Recorded after oxidation of the Mo(IV) complex with Br_2.

The electron-transfer behavior of the MoS_8 complexes is summarized in Scheme I. Waves 1 and 2 are assigned to reversible, metal-centered electron transfers encompassing the Mo(VI), -(V), and -(IV) oxidation states. Waves A and C are assigned to oxidations above or reductions below these levels. These irreversible processes frequently require more than a single electron and probably involve substantial ligand character. The reversibility of waves 1 and 2 infers rapid electron transfer and little structural change for the Mo(VI)/Mo(V) and Mo(V)/Mo(IV) redox couples. Structural determinations have shown the Mo(V) and Mo(IV) complexes Mo(Et_2dtc)$_4$Cl[15] and Mo(Et_2dtc)$_4$[16] to have dodecahedral (DD) and square-antiprismatic (SAP) geometries, respectively. There is little difference in Mo–S bond lengths between the two oxidation states. Molecular orbital analyses[17] show that the DD, SAP, and bicapped trigonal prism are nearly equivalent, energetically favored geometries for eight-coordinate compounds. Thus, a reasonable expectation is that electron transfer among Mo(VI), -(V), and -(IV) species existing in one or more of these forms would involve little structural change and would be rapid and reversible.

Scheme I

$$\text{product} \xleftarrow[(E_p)_A]{-ne^-} Mo^{VI}S_8 \underset{(E_{1/2})_1}{\overset{e^-}{\rightleftharpoons}} Mo^{V}S_8 \underset{(E_{1/2})_2}{\overset{e^-}{\rightleftharpoons}} Mo^{IV}S_8 \xrightarrow[(E_p)_C]{+ne^-} \text{product}$$

EPR and Electronic Spectra. EPR solution spectra of the five Mo(V) complexes contain a strong central line due to the 75% Mo isotopes with $I = 0$ and six hyperfine lines arising from the ^{95,97}Mo isotopes with $I = {}^5/_2$. The isotropic g and A values presented in Table II are consistent with the unpaired electron being located in a metal-centered orbital that has almost constant composition for the entire series of compounds.

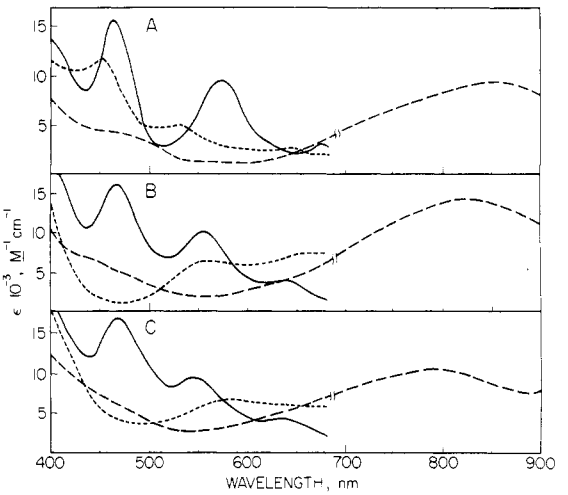

Figure 2. Electronic spectra of Mo(ed)$_4^{n-}$ complexes in 0.2 M (TEA)BF_4/CH_3CN: A, Mo(*i*-mnt)$_4^{2-,3-,4-}$; B, Mo(ced)$_4^{2-,3-,4-}$; C, Mo(ded)$_4^{2-,3-,4-}$; (---) Mo(VI); (—) Mo(V); (···) Mo(IV). Data for Mo(ed)$_4^{2-}$ species at $\lambda > 700$ nm recorded in CH_2Cl_2 after oxidizing the Mo(V) complex with Br_2 or I_2.

This conclusion is supported by Hückel MO calculations of the model dithiocarbamate complex, Mo(H_2dtc)$_4^+$,[7] which describe the HOMO as a molybdenum d_{xy} orbital of >90% metal character. Thus, the EPR results support the interpretation that the Mo(VI)/Mo(V) and Mo(V)/Mo(IV) redox couples are almost totally metal-centered electron transfers. This circumstance may be contrasted with the behavior of molybdenum–tris(1,2-dithiolene) complexes where EPR parameters of $g = 2.009$–2.011 and $A = 11$–12 G indicate greater ligand contribution to the unpaired spin density in the Mo(V) oxidation state.[18,19]

Visible absorption spectra of the ethylenedithiolate complexes are characterized by three charge-transfer bands located at 463–467, 545–572, and 643–672 nm in the Mo(V) oxidation state and a single charge-transfer band located at 670–860 nm in the Mo(VI) oxidation state. As shown in Figure 2 the energies of these transitions increase slightly as the complexes become more difficult to reduce. Spectroscopic data for these compounds are contained in Table V, where correlations between redox potentials and charge-transfer energies are presented. Complete visible absorption data for stable oxidation levels of all the MoS_8 complexes are presented in ref 12.

X-ray Photoelectron Spectra. XPE binding energies for the four complexes isolated as pure Mo(V) salts are presented in Table III. The C 1s energy did not prove to be a suitable reference line, presumably because of the wide variety of functional groups on carbon in these compounds. Instead, binding energies were referenced to an assigned value of 401.1 eV for the N 1s line of the tetraalkylammonium counterions.[20] Values for Mo(Et_2dtc)$_4PF_6$ were related to the other complexes by measuring binding energies relative to the P 2p line of its counterion and applying corrections based on the experimentally measured difference BE(N 1s) − BE(P 2p) = 265.5 eV for the salt *n*-Bu_4NPF_6. The rationality of the above procedure is supported by observations that N 1s binding energies of tetraalkylammonium and other large polarizable ions vary by only a few tenths of 1 eV for a wide range of counterions[20-22] and that prediction of binding energies in transition-metal

(15) Garner, C. D.; Howlader, N. C.; Mabbs, F. E.; McPhail, A. T.; Miller, R. W.; Onan, K. D. *J. Chem. Soc., Dalton Trans.* **1978**, 1582.
(16) van der Aalsvoort, J. G. M.; Beurskens, P. T. *Cryst. Struct. Commun.* **1974**, *3*, 653.
(17) Burdett, J. K.; Hoffmann, R.; Fay, R. C. *Inorg. Chem.* **1978**, *17*, 2553.
(18) Stiefel, E. I. *Prog. Inorg. Chem.* **1977**, *22*, 1 and references therein.
(19) Kwik, W. L.; Stiefel, E. I. *Inorg. Chem.* **1973**, *12*, 2337.
(20) Jack, J. J.; Hercules, D. M. *Anal. Chem.* **1971**, *43*, 729.
(21) Swartz, W. E., Jr.; Ruff, J. K.; Hercules, D. M. *J. Am. Chem. Soc.* **1972**, *94*, 5227.
(22) Jolly, W. L. *Coord. Chem. Rev.* **1974**, *13*, 47.

Table III. Core Electron Binding Energies (eV)[a]

compd	Mo $3d_{5/2}$	S 2p	C 1s	N 1s
$Mo(Et_2dtc)_4PF_6$	229.4 (1.4)	162.0 (2.2)	284.4 (2.9)	399.1 (2.5)[b]
$[n\text{-}Bu_4N]_3Mo(i\text{-}mnt)_4$	229.1 (2.3)	161.4 (2.9)	284.2 (2.7)	397.6 (2.2)[c]
$[n\text{-}Bu_4N]_3Mo(ced)_4$	228.4 (2.8)	161.0 (2.6)	283.8 (2.7)	396.9 (2.1)[c]
$[n\text{-}Pr_4N]_3Mo(ded)_4$	227.9 (1.4)	160.6 (2.3)	284.2 (2.6)	

[a] Binding energies referenced to N 1s = 401.1 eV for R_4N^+ by using procedure described in text; full width at half-maximum given in parentheses. [b] Dithiocarbamate nitrogen. [c] Cyano nitrogen.

Table IV. Correlations of $E_{1/2}$ with Ligand Substituent Parameters

complex[a]	solvent	σ	$(E_{1/2})_1$, V		$(E_{1/2})_2$, V		ref[b]
			ρ	r	ρ	r	
$Mo(S_2CNX_2)_4$ (I)[c,d]	CH_2Cl_2	σ_p	0.083	0.713	0.156	0.802	33
		σ_p^+	0.108	0.604	0.213	0.712	33
		σ_I	0.465	0.988	0.716	0.970	33
		σ^*	0.049	0.970	0.078	0.995	35
$Mo(S_2C_2X_2)_4$ (II)	CH_2Cl_2	σ_p	0.395	0.996	0.399	0.994	33
		σ_p^-	0.395	0.996	0.399	0.994	33
		σ_I	0.395	0.996	0.399	0.994	33
		σ^*	0.063	0.996	0.063	0.994	35
	CH_3CN	σ_p	0.378	0.998	0.364	0.994	33
		σ_p^-	0.378	0.998	0.364	0.994	33
		σ_I	0.378	0.998	0.364	0.994	33
		σ^*	0.060	0.998	0.058	0.994	35
$Mo(S_2CX)_4$ (III)	CH_2Cl_2	σ^*	0.324	0.992	0.223	0.983	36, 37
	CH_3CN	σ^*	0.291	0.985	0.215	0.986	36, 37

[a] Substituent groups: I, $X_2 = (CH_3)_2$, $(C_2H_5)_2$, $(CH(CH_3)_2)_2$, $(CH_3)(CH_2C_6H_5)$, $(CH_2C_6H_5)_2$, $(C_6H_5)_2$; II, $X_2 = (CN)_2$, $(CN)(COOC_2H_5)$, $(COOC_2H_5)_2$; III, $X = SC(CH_3)_3$, $N(C_2H_5)_2$, $^-C(CN)_2$, $^-C(CN)(COOC_2H_5)$, $^-C(COOC_2H_5)_2$. [b] Literature reference for substituent group parameters. [c] Half-wave potential data from ref 6. [d] $X_2 = (C_6H_5)_2$ was omitted from correlations with σ_I and σ^*. Omission of $X_2 = (C_6H_5)_2$ does not improve correlations with σ_p and σ_p^+.

complexes from ligand group shifts is unaffected by differences in molecular charge.[23] The Mo $3d_{5/2}$ and S 2p binding energies corrected on this basis cover a range of ca. 1.5 eV and decrease in the order $Mo(Et_2dtc)_4^+ > Mo(i\text{-}mnt)_4^{3-} > Mo(ced)_4^{3-} > Mo(ded)_4^{3-}$. This sequence parallels the change in $(E_{1/2})_1$ and $(E_{1/2})_2$ for these complexes.

Discussion

Correlation of $E_{1/2}$ with Ligand Substituent Parameters. The most notable electrochemical feature of the MoS_8 complexes is the large change in redox potential imparted by seemingly small changes in ligand structure. The range of reversible half-wave potentials is ~2 V for $(E_{1/2})_2$ and ~1.3 V for $(E_{1/2})_1$ (four complexes). The shifts in these quantities are consistent with the expectation that electron-withdrawing groups favor reduction and electron-donating groups favor oxidation of the complexes. While such large changes in $E_{1/2}$ could be construed to imply substantial ligand character in the electron-transfer orbital,[24] we consider the present case to be a circumstance, similar to previously cited examples,[24-31] wherein a metal-centered redox potential displays a large sensitivity to substitutions on the ligand framework.

In order to better correlate redox potentials with ligand structure, we have plotted half-wave potentials against the sum of ligand substituent parameters according to the relationship[32]

$$E_{1/2} = \rho\sum\sigma + \text{constant} \qquad (1)$$

where ρ is the reaction constant in V. Correlations were attempted with several different types of substituent parameters (σ_p, σ_p^+ or σ_p^-, σ_I, σ^*)[33,34] in an effort to determine whether inductive or resonance factors could be considered to predominate in the transmission of substituent group effects. Results are analyzed in Table IV on the basis of three different ligand frameworks:

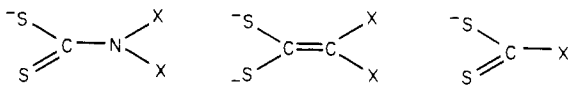

I II III

Structure I represents the alkyl- and aryl-substituted dithiocarbamates studied by Nieuwpoort and Steggerda; we have added correlations with σ_p, σ_p^+, and σ_I to their original correlation[6] with σ^*. Structure II represents the 1,1-ethylenedithiolates. Structure III is used to correlate data for all three types of 1,1-dithio ligands. The successful correlation of shifts in $(E_{1/2})_1$ and $(E_{1/2})_2$ with ligand substituent parameters establishes a basis for predictably adjusting molybdenum-centered redox potentials over a wide range with 1,1-dithio ligands and for understanding the factors responsible for the very considerable effect of ligand structure on these potentials.

The dithiocarbamate complexes show satisfactory correlations with σ_I and σ^* parameters, but not with σ_p and σ_p^+. This expectable result is consistent with inductive charge donation by alkyl groups in structure I. Points for $X = C_6H_5$ do not

(23) Feltham, R. D.; Brant, P. *J. Am. Chem. Soc.* **1982**, *104*, 641.
(24) Patterson, G. S.; Holm, R. H. *Inorg. Chem.* **1972**, *11*, 2285.
(25) Handy, R. F.; Lintvedt, R. L. *Inorg. Chem.* **1974**, *13*, 893.
(26) Patterson, G. S.; Holm, R. H. *Bioinorg. Chem.* **1975**, *4*, 257.
(27) Butler, G.; Chatt, J.; Leigh, G. J.; Pickett, C. J. *J. Chem. Soc., Dalton Trans.* **1979**, 113.
(28) Chum, H. L.; Rock, M. *Inorg. Chim. Acta* **1979**, *37*, 113.
(29) Streeky, J. A.; Pillsbury, D. G.; Busch, D. H. *Inorg. Chem.* **1980**, *19*, 3148.
(30) (a) Kadish, K. M.; Morrison, M. M. *Inorg. Chem.* **1976**, *15*, 980. (b) Walker, F. A.; Beroiz, D.; Kadish, K. M. *J. Am. Chem. Soc.* **1976**, *98*, 3484. (c) Kadish, K. M.; Morrison, M. M.; Constant, L. A.; Dickens, L.; Davis, D. G. *Ibid.* **1976**, *98*, 8387.
(31) Essenmacher, G. J.; Treichel, P. M. *Inorg. Chem.* **1977**, *16*, 800.
(32) Zuman, P. "Substituent Effects in Organic Polarography"; Plenum Press: New York, 1967.
(33) Exner, O. In "Correlation Analysis in Chemistry"; Chapman, N. D., Shorter, J., Eds.; Plenum Press: New York, 1978; Chapter 10.
(34) Very poor correlations were obtained with σ_R, the pure resonance parameter, and these results are not reported.
(35) Taft, R. W., Jr. In "Steric Effects in Organic Chemistry"; Newman, M. S., Ed.; Wiley; New York, 1956; Chapter 13.
(36) Hansch, C.; Leo, A. "Substituent Constants for Correlation Analysis in Chemistry and Biology"; Wiley: New York, 1979.
(37) Hünig, S.; Schenk, W. *Liebigs Ann. Chem.* **1979**, 1523.

Table V. Correlation of Redox Potentials and Charge-Transfer Energies

	Mo(VI)[a]			Mo(V)[b]		
complex	$h\nu_{CT}$, eV	$(E_{1/2})_1$, V	$\lvert(E_{1/2})_1 - (E_p)_A\rvert$, V	$h\nu_{CT}$, eV	$(E_{1/2})_2$, V	$\lvert(E_{1/2})_2 - (E_p)_A\rvert$, V
$Mo(i\text{-mnt})_4^{n-}$	1.44	+0.52	0.99	2.67, 2.17, 1.84	−0.71	2.15
$Mo(ced)_4^{n-}$	1.51	+0.18	0.89	2.65, 2.24, 1.95	−1.02	2.23
$Mo(ded)_4^{n-}$	1.56	−0.30	1.13	2.68, 2.27, 1.94	−1.47	2.27

[a] In CH_2Cl_2. [b] In CH_3CN.

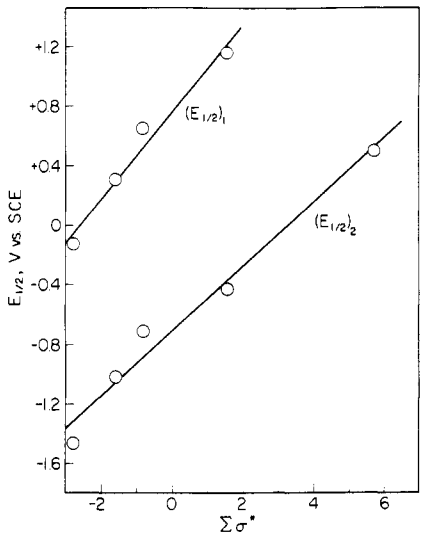

Figure 3. Plots of $(E_{1/2})_1$ and $(E_{1/2})_2$ vs. $\sum\sigma^*$ for substituents X on ligand structure III.

lie on the σ_I and σ^* correlation lines, a result which has been observed previously and attributed to mesomeric interaction of the phenyl group with the ^-S_2CN structure.[6,38] The ethylenedithiolate complexes correlate well with all four parameters, suggesting that substituent effects in structure II are transmitted either by inductive or by combined inductive plus resonance factors. The successful correlation of $(E_{1/2})_1$ and $(E_{1/2})_2$ with $\sum\sigma^*$ on the basis of structure III (Figure 3) relates the redox behavior for all three ligand types and indicates that inductive charge donation by the substituent at the 1,1-dithio site is an important factor in the shifts in $E_{1/2}$. The reaction constants obtained from this correlation are 4–6 times greater than those determined from $E_{1/2}$ vs. $\sum\sigma^*$ plots for structures I and II. The increase is consistent with the locus of substitution being one atom closer to the charge-bearing site in structure III. A similar proportion is found in the definitions of σ^* and σ_I, which are based on the relative rates of hydrolysis of formic and acetic acid esters, i.e., $\sigma^*(X)/\sigma_I(X) = 6.23$.[33]

The values of ρ determined from correlations using σ_p, σ_p^-, and σ_I for structure II and σ_I for structure I are significant. Similarly large reaction constants (ρ = 0.32–0.49) have been obtained from correlations of $E_{1/2}$ with $\sum\sigma_p$ in cases where substituents interact strongly with the reaction site, i.e., directly substituted ferrocenes,[39] ruthenium[24] and chromium[25] acetylacetonate complexes, and substituted aryldiazenide complexes of molydenum.[27] Smaller values of ρ = 0.04–0.08 are noted when substituents are more effectively isolated from the reaction site, as in the case of metal-centered redox reactions of substituted tetraphenylporphyrins[30] and aryl isocyanide complexes of chromium.[31] The observed values of ρ in Table IV indicate very effective transmission of electronic properties from the 1,1-dithio ligand substituents to the site of electron transfer.

Previous discussions[11,38] of the effect of 1,1-dithio ligand structure on the redox potentials of transition metal complexes have emphasized the role of canonical forms IIIa and IIIb in

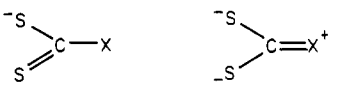

IIIa IIIb

this relationship. This delocalization aids in communicating the electronic properties of the substituent groups to the charge-bearing sites, but the results in Table IV indicate that inductive factors also are important in this regard. Thus, charge density at the sulfur atoms appears to be controlled by a combination of inductive and resonance factors within the ligand. Charge donation from the ligands to the reaction center (Mo atom) must occur principally by inductive means on the basis of the consistently successful correlations of $E_{1/2}$ with $\sum\sigma_I$ and $\sum\sigma^*$ for all three ligand types. This means that the electron-transfer orbital on the Mo atom is not conjugated to the ligand framework through metal–ligand π-bonded forms such as IIIc.[38] A recent ^{13}C NMR investigation of molybdenum(IV) tetrakis(dithiobenzoate) complexes,[40] which finds no evidence for metal-to-ligand or ligand-to-metal delocalization of electron density in these species, is consistent with this assertion.

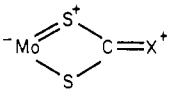

IIIc

Correlation of $E_{1/2}$ with Spectroscopic Properties. Because absorption spectroscopy probes electronic structure, correlations between redox potentials and electronic absorption energies frequently are sought for organic and inorganic compounds. Two approaches have been followed: the electronic transition energy may be compared directly to a single redox potential[41] or to a difference between two potentials.[42] Successful correlations of the former type have been reported for organic donor–acceptor complexes,[41a] boron-containing adducts of dicyanobis(1,10-phenanthroline)iron(II),[43] and iron–diimine complexes.[28] The latter approach has been used successfully to treat metal-to-ligand CT bands in transition-metal tris(bipyridine) complexes[42] and singlet and triplet absorptions in aza heterocyclic and aromatic hydrocarbons.[44] We include both approaches in our consideration of CT absorptions by the MoS_8 complexes.

(38) Chant, R.; Hendrickson, A. R.; Martin, R. L.; Rohde, N. M. *Inorg. Chem.* **1975**, *14*, 1894.
(39) (a) Hoh, G. L. K.; McEwen, W. E.; Kleinberg, J. *J. Am. Chem. Soc.* **1961**, *83*, 3949. (b) Little, W. F.; Reilley, C. N.; Johnson, J. D.; Sanders, A. P. *Ibid.* **1964**, *86*, 1382. (c) Hall, D. W.; Russell, C. D. *Ibid.* **1967**, *89*, 2316.
(40) Roberie, T.; Bhacca, N. S.; Lankin, D.; Selbin, J. *Can. J. Chem.* **1980**, *58*, 2314.
(41) (a) Peover, M. E. In "Electroanalytical Chemistry"; Bard, A. J., Ed.; Marcel Dekker: New York, 1967; Vol. 2, pp 1–51. (b) Vlcek, A. A. *Electrochim. Acta* **1968**, *13*, 1063.
(42) Saji, T.; Aoyagui, S. *J. Electroanal. Chem. Interfacial Electrochem.* **1975**, *60*, 1.
(43) Shriver, D. F.; Posner, J. *J. Am. Chem. Soc.* **1966**, *88*, 1672.
(44) Loutfy, R. O.; Loutfy, R. O. *Can. J. Chem.* **1976**, *54*, 1454.

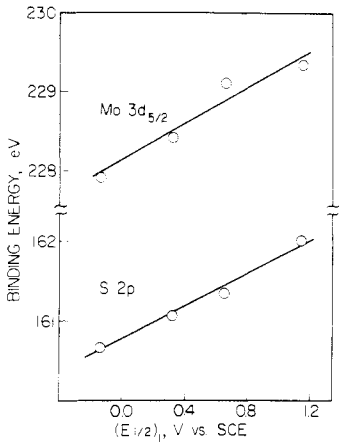

Figure 4. Dependence of Mo $3d_{5/2}$ and S 2p binding energies on the Mo(VI)/Mo(V) redox potential. Equations of the lines are BE = $1.221(E_{1/2})_1 + 228.1$ ($r = 0.9786$) for Mo $3d_{5/2}$ and BE = $1.096(E_{1/2})_1 + 160.7$ ($r = 0.9979$) for S 2p.

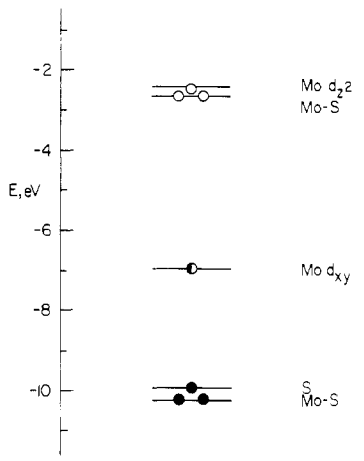

Figure 5. Molecular orbital energy levels in $Mo(H_2dtc)_4^+$ from ref 5 and 7.

Redox and spectroscopic data for the ethylenedithiolate complexes, $Mo(ed)_4^{n-}$ ($n = 2$ or 3), are summarized in Table V. Direct comparison of $h\nu_{CT}$ with $E_{1/2}$ yields satisfactory correlations for the Mo(VI) band and for the second Mo(V) band. The charge-transfer energies increase as reduction of the complex becomes more difficult. This result is consistent with LMCT, which is the expected direction of the spectroscopic transition in the case of the d^0 Mo(VI) complexes. However, the total range of $h\nu_{CT}$ values is small in comparison to the range of $E_{1/2}$ values.

Charge-transfer energies are compared to redox potential differences using Aoyagui's model.[42] Since ligand reduction potentials ($(E_p)_C$ in Scheme I) are unavailable for two of the three ed complexes, it is possible to make comparisons only on the basis of ligand-to-metal charge transfer:

$$h\nu_{LMCT} = |(E_{1/2})_M^{red} - (E_{1/2})_L^{ox}| + (\text{constant}) \quad (2)$$

In eq 2 $(E_{1/2})_M^{red}$ is the reduction potential of the metal center, $(E_{1/2})_1$ or $(E_{1/2})_2$, and $(E_{1/2})_L^{ox}$ is the oxidation potential of the ligand center, $(E_p)_A$.[45] Correspondence between $h\nu_{LMCT}$ and the redox potential differences is satisfactory only for the two low-energy Mo(V) CT bands. We conclude that neither of the two procedures for comparing $h\nu_{CT}$ with redox potentials in Table V is fully successful. This appears to be due to the fact that electronic spectral properties of the $Mo(ed)_4^{n-}$ complexes experience only small changes with ligand structure in comparison to electrochemical ones.

In order to investigate further possible relationships between electrochemical and spectroscopic properties and to test our interpretation of the effect of ligand structure on redox potentials, we measured Mo 3d and S 2p XPE binding energies for the four isolated Mo(V) salts. Because binding energies and redox potentials both respond to changes in charge density and because no large structural differences are anticipated among the MoS_8 complexes, a direct relationship between BE and $E_{1/2}$ might be expected for this set of compounds. Figure 4 illustrates the excellent correlation found between the Mo(VI)/Mo(V) redox potential and the Mo $3d_{5/2}$ and S 2p binding energies. In accordance with expectations, the Mo 3d binding energies increase as $E_{1/2}$ becomes more positive. Sulfur 2p binding energies increase in a parallel manner. This observation apparently reflects the tendency of the two bonded atoms to distribute charge more or less equally between one another. Thus, Mo 3d and S 2p BE's rise and fall together in response to the amount of negative charge donated to the Mo–S site by the electronic character of the ligand.

A successful correlation of XPE binding energies with redox potentials also has been reported[46] for a series of (tetraphenylporphyrin)iron(III) complexes, FeTPPX, wherein the coordinated ion $X^- = Cl^-$, Br^-, N_3^-, or ClO_4^- controls charge density at the metal site. Further BE–$E_{1/2}$ correlations should exist in transition-metal chemistry provided structural and bonding properties are maintained acceptably constant within a series of compounds. The concepts underlying such a relationship are embodied in the recent development of empirical ligand group shifts for predicting XPE binding energies.[23]

Relationships among Electrochemical, Spectroscopic, and Structural Properties. The relationships we have observed between half-wave potentials and XPE, CT absorption, and EPR spectroscopic parameters and the extent to which these properties are influenced by changes in ligand structure are interpretable from the molecular orbital diagram shown in Figure 5. This diagram is adapted from extended Hückel calculations of the model molybdenum(V) dithiocarbamate complex, $Mo(H_2dtc)_4^+$.[5,7] It is assumed to be qualitatively applicable to the entire series of MoS_8 complexes because of the probable structural similarity of these compounds.[17] More extensive calculations of electronic structure are being undertaken for all five MoS_8 complexes, and a more quantitative interpretation based on the results of these calculations will be presented subsequently.[47]

The diagram in Figure 5 shows a molybdenum d_{xy} orbital of almost pure metal character isolated between filled bonding and empty antibonding orbitals of mixed Mo and S character. The Mo(VI)/Mo(V) and Mo(V)/Mo(IV) redox couples identified in Scheme I are assigned to reversible electron transfers involving this d_{xy} orbital. Oxidation above the Mo(VI) level requires removal of electrons from bonding orbitals, while reduction below the Mo(IV) level involves addition of electrons to antibonding orbitals. These processes are observed as the irreversible and frequently multielectronic waves A and C in Scheme I.

When changes are made in ligand structure that influence the amount of negative charge present at the S atoms, the entire manifold of orbitals in Figure 5 moves up or down in energy. However, for compounds of similar structure the spacings between the levels would be expected to remain relatively constant. Therefore, XPE binding energies and

(45) While use of reversible potentials for $(E_{1/2})_L^{ox}$ in eq 2 is desirable, only the irreversible potentials $(E_p)_A$ are available to us. However, we have used potentials for oxidation of the coordinated- rather than free-ligand center, because we note that the correlations in ref 42 are improved if similar data are used.

(46) Kadish, K. M.; Bottomley, L. A.; Brace, J. G.; Winograd, N. *J. Am. Chem. Soc.* **1980**, *102*, 4341.

(47) Perkins, P. G.; Schultz, F. A., submitted for publication in *Inorg. Chem.*

electrochemical half-wave potentials, which reflect the energy of a single orbital, show a substantial dependence on ligand structure and correlate well one another. Charge-transfer energies, which reflect a difference in energy between two orbitals, remain approximately constant and do not correlate well with $E_{1/2}$ or binding energy. A similar rationale,[48] citing the spherical component of the ligand field potential as the principal factor determining the energy of a metal orbital, has been proposed to explain the general lack of correlation between $E_{1/2}$ and Dq for transition-metal compounds. A similar argument appears to be applicable in the case of charge-transfer transitions for MoS_8 complexes.

The molecular orbital description of $Mo(H_2dtc)_4^+$ also indicates that the charge donated from ligand to metal, which controls the $E_{1/2}$'s and BE's, does so through Mo–S bonding orbitals that are not involved in the metal-centered redox processes. Thus, large changes in $(E_{1/2})_1$ and $(E_{1/2})_2$ with ligand structure do not necessarily imply substantial ligand character in the electron-transfer act. Finally, the relative constancy of the EPR parameters in Table II indicates that the character of the Mo d_{xy} orbital changes very little as it moves up or down in energy. As demonstrated previously[49] electronic charge and electron spin density are independent properties and may be manifested in different experimental measurements.

Acknowledgment. Support of this research by the National Science Foundation under Grant No. CHE 80-20442 is gratefully acknowledged. We also wish to thank Dr. P. Brandt for a preprint of ref 23 and Professors A. Lombardo, K. Kadish, and R. Dessy for constructive comments.

Registry No. $Mo(Et_2dtc)_4PF_6$, 81655-19-8; $[n\text{-}Bu_4N]_3Mo(i\text{-}mnt)_4$, 81643-67-6; $[n\text{-}Bu_4N]_3Mo(ced)_4$, 81642-88-8; $[n\text{-}Pr_4N]_3Mo(ded)_4$, 81642-90-2; $Mo(t\text{-}Butxn)_4^+$, 81625-82-3; $Mo(Et_2dtc)_4^+$, 51155-43-2; $Mo(i\text{-}mnt)_4^{3-}$, 81643-66-5; $Mo(ced)_4^{3-}$, 81642-87-7; $Mo(ded)_4^{3-}$, 81642-89-9; $Mo(ced)_4^{2-}$, 81643-65-4; $Mo(i\text{-}mnt)_4^{2-}$, 81643-64-3; $Mo(ded)_4^{2-}$, 81643-63-2; $Mo(ced)_4^{4-}$, 81643-62-1; $Mo(i\text{-}mnt)_4^{4-}$, 81643-61-0; $Mo(ded)_4^{4-}$, 81643-60-9.

(48) Lintvedt, R. L.; Fenton, D. E. *Inorg. Chem.* **1980**, *19*, 569.

(49) (a) Dessy, R. E.; Charkoudian, J. C.; Abeles, T. P.; Rheingold, A. L. *J. Am. Chem. Soc.* **1970**, *92*, 3947. (b) Dessy, R. E.; Charkoudian, J. C.; Rheingold, A. L. *Ibid.* **1972**, 94, 738.

Contribution from the School of Chemical Sciences, University of Illinois—Urbana-Champaign, Urbana, Illinois 61801

Nitrogen-14 Nuclear Quadrupole Resonance Spectra of Metal Anthranilate Complexes[1]

D. ANDRÉ D'AVIGNON and THEODORE L. BROWN*

Received December 4, 1981

The ^{14}N nuclear quadrupole resonance (NQR) spectra at 77 K have been obtained for solid divalent metal ion complexes ML_2 of the anthranilate anion, $L = CO_2C_6H_4NH_2^-$, where M = Zn, Cd, Hg, Pd(II), Ca, Mg, Ba, Sr, Pb, and Sn(II), and for $Hg(CO_2C_6H_4NH_2)Cl$. The ^{14}N NQR data permit the evaluation of the quadrupole coupling constant $e^2q_{zz}Q/h$ and asymmetry parameter η, the two independent components of the electric field gradient tensor at nitrogen, in all the complexes. The NQR data can be interpreted in terms of a coordinated nitrogen model, on the basis of a modified Townes–Dailey analysis, to yield an estimate of the extent of withdrawal of electronic charge from nitrogen in the metal ion complexes, as compared with that of the protonated amino group as reference compound. The results show that electron withdrawal varies in the order Hg > Pd >> Sn > Pb > Cd ≈ Zn > Ca ≈ Mg > Sr > Ba. The results for the $Hg(CO_2C_6H_4NH_2)_2$ complex are anomalous, suggesting that the electronic environment about nitrogen is different in this complex than that in the others.

Anthranilic acid (*o*-aminobenzoic acid) forms complexes of 2:1 stoichiometry with a variety of divalent metal ions. These complexes have been of interest as potential antiinflammatory drugs, as potential hydrogenation catalysts, as antioxidants in films, and as bond strengtheners in epoxy adhesives.[2-5]

The anthranilate anion acts as a bidendate ligand; coordination occurs through the amino nitrogen and the carboxylato oxygen. The copper[6] and yttrium[7] complexes have been the subjects of crystal structure determinations. In the divalent copper complex the arrangement about the metal center is distorted octahedral. Two anthranilate ligands occupy planar positions in a trans configuration about the metal, while the axial positions are occupied by carbonyl oxygens of the ligands on adjacent complexes. This structure is similar to that found for the glycine–cadmium complex.[8] IR and magnetic measurements suggest that the structures of other bis(anthranilato)metal complexes are similar to that of the copper complex.

The work reported here represents a continuation of previous nuclear quadrupole resonance (NQR) studies of metal–nitrogen interactions.[9-13] Our major concern is to examine the manner in which coordination of the amino group nitrogen to the metal center affects the electron distribution about the

(1) This research was supported by Research Grant GM-23395 from the Institute of General Medical Sciences, National Institutes of Health.
(2) Sorenson, J. R. J. *J. Med. Chem.* **1976**, *19*, 135.
(3) Holy, N. L. *Fundam. Res. Homogeneous Catal.* **1979**, *3*, 691.
(4) Hoshino, M.; Matsumoto, T. Japan Kokai Tokkyo Koho 76 128,331 (Cl. CO9D5/08), Nov 9, 1976 (*Chem. Abstr.* **1977**, *86*, 74538*d*).
(5) Umehara, K.; Ohnishi, Y.; Kira, T. *Aichi-ken Kogyo Shidosho Hokoku* **1978**, *14*, 54.
(6) Lange, B. A.; Haendler, H. M. *J. Solid State Chem.* **1975**, *15*, 325.
(7) Boudreau, S. M.; Haendler, H. M. *J. Solid State Chem.* **1981**, *36*, 190–194.
(8) Low, B. N.; Hirshfeld, F. L.; Richards, F. M. *J. Am. Chem. Soc.* **1959**, *81*, 4412.
(9) Rubenacker, G. V.; Brown, T. L. *Inorg. Chem.* **1980**, *19*, 392.
(10) Ashby, C. I. H.; Cheng, C. P.; Brown, T. L. *J. Am. Chem. Soc.* **1978**, *100*, 6057.
(11) Ashby, C. I. H.; Cheng, C. P.; Duesler, E. N.; Brown, T. L. *J. Am. Chem. Soc.* **1978**, *100*, 6063.
(12) Brown, T. L. *J. Mol. Struct.* **1980**, *58*, 293.
(13) Ashby, C. I. H.; Paton, W. F.; Brown, T. L. *J. Am. Chem. Soc.* **1980**, *102*, 2990.

0020-1669/82/1321-3041$01.25/0 © 1982 American Chemical Society